

*Physics*  
*Physics fields*

---

Okayama University

Year 2005

---

Fabrication of a logic gate circuit based  
on ambipolar field-effect transistors with  
thin films of C<sub>60</sub> and pentacene

Eiji Kuwahara\*      Haruka Kusai†      Takayuki Nagano‡  
Toshio Takayanagi\*\*      Yoshihiro Kubozono Prof.††

\*Okayama University

†Okayama University

‡Okayama University

\*\*Okayama University

††Okayama University, [kubozono@cc.okayama-u.ac.jp](mailto:kubozono@cc.okayama-u.ac.jp)

This paper is posted at eScholarship@OUDIR : Okayama University Digital Information Repository.

[http://escholarship.lib.okayama-u.ac.jp/physics\\_general/5](http://escholarship.lib.okayama-u.ac.jp/physics_general/5)

Fabrication of a logic gate circuit based on ambipolar field-effect transistors with  
thin films of C<sub>60</sub> and pentacene

Eiji Kuwahara, Haruka Kusai, Takayuki Nagano, Toshio Takayanagi,  
Yoshihiro Kubozono\*

*Department of Chemistry, Okayama University, Okayama 700-8530, Japan  
and CREST, Japan Science and Technology Agency, Kawaguchi, 322-0012,  
Japan*

Received 17 February 2005; in final form xx June 2005

**Abstract**

Ambipolar field-effect transistor (FET) devices were fabricated with a heterostructure of C<sub>60</sub> and pentacene, and their p- and n-channel field-effect mobilities were studied as a function of thickness of pentacene thin-films. The observed dependences of the  $\mu$  values were interpreted in terms of the morphology of the thin films and the band structure of C<sub>60</sub>/pentacene heterostructure. A complementary metal-oxide-semiconductor (CMOS) circuit was fabricated by integration of two ambipolar FETs, aiming at realization of a new CMOS inverter circuit composed of FETs with the same device structure. The gain of 4, the threshold voltage of 85 V, and the complex output characteristics were explained on the basis of the properties of the component FET devices.

Corresponding author. FAX: +81-86-251-7853.

E-mail address: kubozono@cc.okayama-u.ac.jp (Y. Kubozono).

## 1. Introduction

Field-effect transistors (FETs) with thin films of fullerenes have been extensively studied owing to their potential applications towards next-generation electronic devices [1-10]. The fullerene FET device, first fabricated with thin films of C<sub>60</sub> by Haddon et al. [1], showed n-channel properties with a field-effect mobility  $\mu$  of 0.08 – 0.30 cm<sup>2</sup> V<sup>-1</sup> s<sup>-1</sup>, and it was raised to 0.56 cm<sup>2</sup> V<sup>-1</sup> s<sup>-1</sup> by a recent measurement of FET-properties under 10<sup>-9</sup> Torr [4]. The highest  $\mu$  value among the p-channel FETs with thin-films of organic molecules is 1.5 cm<sup>2</sup> V<sup>-1</sup> s<sup>-1</sup> in a pentacene FET [11].

A combination of two independent C<sub>60</sub> and pentacene FET devices led to a complimentary metal-oxide-semiconductor (CMOS) inverter circuit [5]. The CMOS circuits are incorporated into various types of chips such as memories and microprocessors owing to their low-power consumption, good-noise margin and ease of design [12,13]. The importance of CMOS logic gate circuits lies in the FET devices with thin films of organic molecules, which enable realization of computer chips with flexibility, portability, and shock-resistance. An ambipolar FET device with a heterostructure of C<sub>60</sub> and pentacene that we have recently fabricated showed  $\mu$  values as high as 10<sup>-3</sup> – 10<sup>-2</sup> cm<sup>2</sup> V<sup>-1</sup> s<sup>-1</sup> [10]. For further application of these CMOS circuits, simpler and easier processes for fabrication are needed, and one of the possibilities is a proper use of ambipolar FET devices as their components, because such a circuit can be realized with only one type of ambipolar FET device.

The present letter reports on our measurement of the dependence of the  $\mu$  values on the thickness of pentacene thin-films in C<sub>60</sub>/pentacene heterostructure FET devices in order to

clarify the relationship between the device structure and the ambipolar properties. Furthermore, we have fabricated a CMOS inverter circuit by integration of two ambipolar FETs on SiO<sub>2</sub>/Si substrate to study the output characteristics of the inverter circuit based on their FET properties.

## 2. Experimental

Schematic representations of heterostructure FET devices of C<sub>60</sub> and pentacene are shown in Fig. 1. All FET devices fabricated take the middle-contact device structure. Details of fabrication of the FET device were described elsewhere [10]. The channel length  $L$  and the channel width  $W$  of the device were 30 and 2500  $\mu\text{m}$ , respectively. The characteristics of the FET devices and CMOS inverter circuit were measured at  $10^{-6}$  Torr and 300 K. The FET properties were measured in the p- and n-channel measurement modes shown in Fig. 2(a). The absolute value of the leak current produced by applying the gate voltage  $V_G$ ,  $|I_G|$ , was always below 0.2 pA at  $|V_G| < 120$  V. The  $I_G$  never affected the drain current,  $I_D$ , and the insulating behavior of SiO<sub>2</sub> was steadily maintained. The diffusion of C<sub>60</sub> and pentacene into the SiO<sub>2</sub> layer by annealing was deemed negligible, because  $|I_G| < 0.2$  pA after annealing of the device at 140 °C for 6 d.

## 3. Results and discussion

### 3.1. $I_D$ - $V_{DS}$ plots of C<sub>60</sub>/pentacene heterostructure FET device

Plots of the  $I_D$  vs. drain-source voltage  $V_{DS}$  for the C<sub>60</sub>/pentacene heterostructure FET device (Fig. 1(a)) are shown in Figs. 2(b) and (c). In the p-channel mode, the  $|I_D|$  increases

supra-linearly with increasing  $|V_{DS}|$  at low values of  $|V_G|$ , and it decreases with increasing  $|V_G|$  up to 30 V, as shown in Fig. 2(b). The  $I_D - V_{DS}$  plots show typical p-channel enhancement FET properties at high  $|V_G|$ . In the n-channel mode, the  $I_D$  increases supra-linearly with increasing  $V_{DS}$  at low values of  $V_G$  (Fig. 2(c)). The  $I_D$  decreases with increasing  $V_G$  and reaches a minimum value at  $|V_G| \approx 50$  V. Further increase in  $|V_G|$  leads to the enhancement of  $I_D$ , and the  $I_D - V_{DS}$  plots show n-channel properties (Fig. 2(c)). The p- and n-channel field-effect mobilities,  $\mu_p$  and  $\mu_n$ , are estimated to be  $3.7 \times 10^{-2}$  and  $5.8 \times 10^{-3}$   $\text{cm}^2 \text{V}^{-1} \text{s}^{-1}$ , respectively, using the general formula for the linear region [13]. Thus, the ambipolar FET properties are observed in the device structure shown in Fig. 1(a).

The energy levels of Au/pentacene/ $C_{60}$ , shown in Fig. 3(a), are drawn following Refs. [14] and [15]. The Fermi level,  $\varepsilon_F$ , is very close to the valence band of pentacene, while the  $\varepsilon_F$  is also close to that of the conduction band of  $C_{60}$ . Therefore, the injection probability of the hole in pentacene should be higher than that of electron, leading to the p-type behavior in the pentacene thin-films. On the other hand, the injection probability of electron in  $C_{60}$  should be higher than that of the hole. This leads to the n-type behavior in the  $C_{60}$  thin-films. Consequently, the ambipolar FET property in the  $C_{60}$ /pentacene heterostructure FET device originates from the n-channel conduction in the  $C_{60}$  thin-films and the p-channel conduction in the pentacene thin-films.

The pentacene/ $C_{60}$  FET device (Fig. 1(b)) also exhibited ambipolar FET properties after annealing. The  $\mu_p$  and  $\mu_n$  values were  $3.1 \times 10^{-5}$  and  $1.9 \times 10^{-3}$   $\text{cm}^2 \text{V}^{-1} \text{s}^{-1}$ , respectively. This  $\mu_p$  value of the present FET device was smaller by three orders of magnitude than that in the FET device shown in Fig. 1(a). This observation can be accounted for by the fact that

the bottom-contact type pentacene FET exhibits lower FET properties than the top contact-type FET.

### *3.2. Thickness dependence of $\mu_p$ and $\mu_n$ in $C_{60}$ /pentacene heterostructure FET device*

The dependences of  $\mu_p$  and  $\mu_n$  on the thickness of pentacene in the  $C_{60}$ /pentacene heterostructure FET device (Fig. 1(a)) are shown in Fig. 3(b); the thickness of  $C_{60}$  thin-films was fixed to 80 nm for all the samples. The FET devices without annealing showed only p-channel properties, and the  $\mu_p$  was independent of the thickness of the pentacene thin-film. The  $\mu_p$  for the FET devices with smaller thickness of pentacene than 20 nm decreases rapidly by annealing the device at 120 °C for 18 h, as shown in Fig. 3(b). This decrease can be explained by the assumption that the pentacene grains are sparsely distributed in the channel region by sublimation of pentacene by annealing. The sublimed pentacene seems to be intercalated into the spatial sites of  $C_{60}$  thin-films on the pentacene thin-films. The sparse distribution of pentacene grains suppresses the hopping of the carriers between the crystalline grains because of a decrease in the overlap between the orbitals, leading to the lowering of the  $\mu_p$ . No such sparse distribution of pentacene occurs in the channel region of the FET devices with larger thickness of pentacene thin-films even if parts of pentacene were sublimed by annealing, i.e., the  $\mu_p$  should not decrease in the FET device. Actually, the  $\mu_p$  value remained almost constant before and after the annealing of the FET device with large thickness of pentacene thin-films.

The  $\mu_p$  value of the FET device after the annealing decreases with decreasing the thickness of pentacene thin-films below 25 nm, as shown in Fig. 3(b). The  $\mu_p$  value is

leveled above 25 nm. The pentacene grains should be more sparsely distributed because of the sublimation caused by the annealing, when the thickness of the pentacene thin-films is decreased. This should lead to the decrease in the  $\mu_p$  value.

The annealing produced the n-channel FET properties in the FET device. The n-channel properties are associated with the  $C_{60}$  thin-films. The  $\mu_n$  value shows a maximum in the FET device with 25 nm thickness of pentacene, and the  $\mu_n$  decreases by one order of magnitude in the FET device with 17 nm thickness of pentacene. This finding is ascribed to the lowered flatness of interface between the thin-films of pentacene and  $C_{60}$  owing to the intercalation of pentacene into the spatial sites of the  $C_{60}$  thin-films. The low flatness should lead to the trapping of electron carriers. On the other hand, the  $\mu_n$  value decreases by one order of magnitude when the thickness of pentacene increases to 40 nm. As seen from Fig. 3(c), the large accumulation of electron occurs in the channel region of the  $C_{60}$  thin films caused by a large band bending when the thickness of the pentacene thin-films is small, while only small accumulation of electrons is expected owing to a small band bending when the thickness is larger. If this is the case, the  $V_T$  in the n-channel operation should increase with increasing thickness of pentacene. In fact, the  $V_T$  increases from 100 to 180 V with increasing thickness from 25 to 40 nm. Thus, the lowering of the field effect on the  $C_{60}$  thin-films due to the large thickness of pentacene leads to the decrease in the  $\mu_n$ .

### 3.3. CMOS inverter circuits composed of two $C_{60}$ /pentacene heterostructure FET devices

A CMOS inverter circuit was fabricated with two ambipolar  $C_{60}$ /pentacene FETs (Fig. 1(a)). A schematic representation and a picture of the circuit are shown in Figs. 4(a) and (b), respectively. Two FETs are named devices I and II, as shown in Fig. 4(a). The plots of  $I_D$ –

$V_{DS}$  were measured individually for these devices in the normal p- and n-channel measurement modes (Fig. 2(a)). The  $\mu_p$  and  $\mu_n$  values for device I were  $3.1 \times 10^{-1}$  and  $2.3 \times 10^{-5} \text{ cm}^2 \text{ V}^{-1} \text{ s}^{-1}$ , respectively, while those for device II were  $3.1 \times 10^{-1}$  and  $4.0 \times 10^{-5} \text{ cm}^2 \text{ V}^{-1} \text{ s}^{-1}$ , respectively. The  $I_D - V_{out}$  plots for these devices are shown in Fig. 4(c). The  $I_D - V_{out}$  plots were obtained from the  $I_D - V_{DS}$  plots in the p-channel mode for device I, and from the  $I_D - V_{DS}$  plots in the n-channel mode for device II. The  $V_{out} - V_{in}$  plot (Fig. 5(a)) can be predicted for this inverter circuit from the intercepts of the  $I_D - V_{out}$  plots (Fig. 4(c)) for these devices at the same  $V_{in}$  value. The predicted  $I_D - V_{out}$  plot (Fig. 5(a)) shows a rapid decrease in  $V_{out}$  at high  $V_{in}$ .

As shown in Fig. 4(a), the source of device II is grounded, while that of device I is connected to a power supply,  $V_{DD}$ , of 120 V. The experimental output characteristics shown in Fig. 5(b) were measured by the way represented in Fig. 4(a). The consistency between the predicted (Fig. 5(a)) and the experimental (Fig. 5(b)) output characteristics implies that these two FET devices operate properly in this CMOS circuit. The  $V_{out}$  value of  $\approx 90$  V at  $V_{in} < 80$  V was observed, while the  $V_{out}$  of  $\sim 30$  V was observed at  $V_{in} > 90$  V. Thus, no vanishing of  $V_{out}$  was observed in this CMOS circuit even at high  $V_{in}$ . This feature can be ascribed to the fact that neither device I nor II is ever fully switched off because the CMOS circuit consists of two ambipolar FETs, as in the CMOS circuits reported in Ref. [7]. The gain and the threshold voltage of this circuit,  $V_{TIC}$ , were 4 and 85 V, respectively. This high  $V_{TIC}$  originates from the threshold voltage  $|V_{Tp}|$  of 46 V for the p-channel FET property in device I, and the high threshold voltage  $V_{Tn}$  of 51 V for the n-channel FET property in device II. In this case, the  $V_{TIC}$  is expected to lie between 51 and 74 V.

The CMOS circuits with the same ambipolar FETs are expected to be useful for a simple and low-cost fabrication process of electronic devices, although the use of ambipolar FET devices leads to a lowering of gain because of a background current flowing through this circuit. A slight increase in  $V_{out}$  was observed with increasing  $V_{in}$  at  $V_{in} < 80$  V. This finding directly reflects the fact that depletion of the hole occurs in device II at  $V_{in} < 70$  V. Furthermore, a slight increase was observed again at  $V_{in} > 110$  V being due to the depletion of electron in device I. The  $V_{out}$  and  $V_{in}$  values in this circuit are high because of the low  $C_0$  and the thick layer (420 nm) of  $SiO_2$ . Such high values of  $V_{out}$  and  $V_{in}$  should be decreased by using either a high  $\epsilon_x$  or a very thin insulating layer.

#### Acknowledgment

This work was partly supported by Mitsubishi Foundation and a Grant-in-Aid (15350089) of Ministry of Education, Culture, Sports, Science and Technology of Japan.

#### References

- [1] R.C. Haddon, A.S. Perel, R.C. Morris, T.T.M. Palstra, A.F. Hebard, R.M. Fleming, Appl. Phys. Lett. 67 (1995) 121.
- [2] A. Dodabalapur, H.E. Katz, L. Torsi, R.C. Haddon, Science 269 (1995) 1560.
- [3] R.C. Haddon, J. Am. Chem. Soc. 118 (1996) 3041.
- [4] S. Kobayashi, T. Takenobu, S. Mori, A. Fujiwara, Y. Iwasa, Appl. Phys. Lett. 82 (2003) 4581.
- [5] T. Kanbara, K. Shibata, S. Fujiki, Y. Kubozono, S. Kashino, T. Urisu, M. Sakai, A. Fujiwara, R. Kumashiro, K. Tanigaki, Chem. Phys. Lett. 379 (2003) 223.

- [6] S. Kobayashi, S. Mori, S. Iida, H. Ando, T. Takenobu, Y. Taguchi, A. Fujiwara, A. Taninaka, H. Shinohara, Y. Iwasa, *J. Am. Chem. Soc.* 125 (2003) 8116.
- [7] E. J. Meijer, D.M. De Leeuw, S. Setayesh, E. van Veenendaal, B.-H. Huisman, P.W. M. Blom, J.C. Hummelen, U. Scherf, T.M. Klapwijk, *Nature Mater.* 2 (2003) 678.
- [8] Y. Kubozono, Y. Rikiishi, K. Shibata, T. Hosokawa, S. Fujiki, H. Kitagawa, *Phys. Rev. B* 69 (2004) 165412.
- [9] K. Shibata, Y. Kubozono, T. Kanbara, T. Hosokawa, A. Fujiwara, Y. Ito, H. Shinohara, *Appl. Phys. Lett.* 84 (2004) 2572.
- [10] E. Kuwahara, Y. Kubozono, T. Hosokawa, T. Nagano, K. Masunari, A. Fujiwara, *Appl. Phys. Lett.* 85 (2004) 4765.
- [11] Y.-Y. Lin, D.J. Gundlach, S.F. Nelson, T.N. Jackson, *IEEE Electron Device Lett.* 18 (1997) 606.
- [12] S.-M. Kang and Y. Leblebici, *CMOS Digital Integrated Circuits, Analysis and Design*, Mc-Graw Hill, New York, 2003.
- [13] S.M. Sze, *Semiconductor Devices, Physics and Technology*, Wiley, New York, 2002.
- [14] M. Shiraishi, K. Shibata, R. Maruyama, M. Ata, *Phys. Rev. B* 68 (2003) 235414.
- [15] P.G. Schroeder, C.B. France, J.B. Park, B.A. Parkinson, *J. Appl. Phys.* 91 (2002) 3010.

## Figure captions

Fig. 1. Cross sectional views of C<sub>60</sub>/pentacene FET devices. (a) A thin film of C<sub>60</sub> is deposited on a thin film of pentacene, and (b) a thin film of pentacene is deposited on a thin film of C<sub>60</sub>.

Fig. 2. (a) Schematic representation of p- and n-channel measurement circuits.  $I_D - V_{DS}$  plots of the C<sub>60</sub>/pentacene heterostructure FET device measured in (b) the p-channel measurement-mode and (c) the n-channel measurement mode. The FET device was annealed at 140 °C for  $\approx 6$  d under vacuum of  $10^{-6}$  Torr before the measurements of FET properties.

Fig. 3. (a) Energy band diagrams of the C<sub>60</sub>, pentacene and Au electrode. (b) Dependences of  $\mu_p$  and  $\mu_n$  on the thickness of pentacene thin-films for the C<sub>60</sub>/pentacene FET device. ●:  $\mu_p$  before the annealing of the device. ◆:  $\mu_p$  and ■:  $\mu_n$  after the annealing of the device at 120 °C for 18 h. (c) Band bending of energy levels in the FETs with different thicknesses of pentacene thin-films at positive  $V_G$ .

Fig. 4. (a) Schematic representation and (b) picture of CMOS inverter circuit. (c)  $I_D - V_{out}$  plots for devices I and II after the annealing of the CMOS chip at 140 °C for 18 h, where  $V_G = V_{in} - V_{DD}$  and  $V_{DS} = V_{DD} - V_{out}$  for device I, and  $V_G = V_{in}$  and  $V_{DS} = V_{out}$  for device II. Very low- $I_D$  region is shown to clarify the properties at high  $V_{in}$

in the right figure of (c), where plots drawn with the same color correspond to those for the same  $V_{in}$ , and the intercepts at the same  $V_{in}$  are drawn by large closed circles.

Fig. 5. (a) Theoretical  $V_{out} - V_{in}$  plot obtained from the intercepts of the  $I_D - V_{out}$  plots shown in Fig. 4(c). (b)  $V_{out} - V_{in}$  plot measured for the CMOS inverter after the annealing at 140 °C for 18 h. The  $V_{out} - V_{in}$  plot shown in (b) was directly measured using the circuit shown in Fig. 4(a).

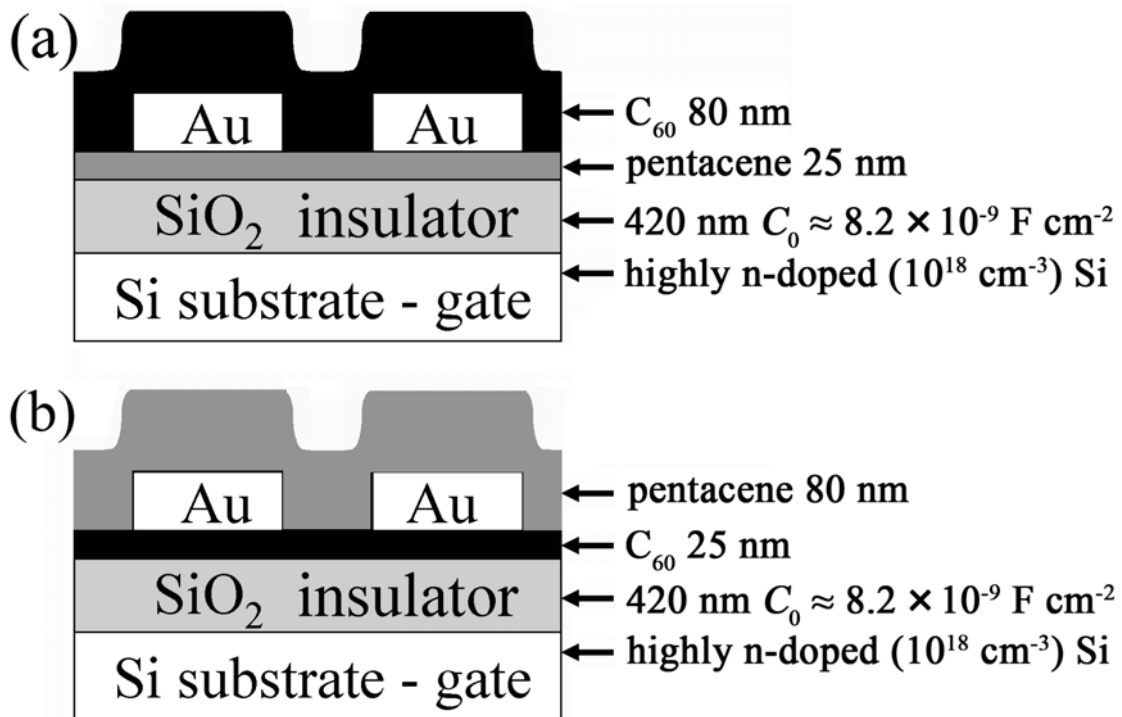


Fig. 1. E. Kuwahara et al.

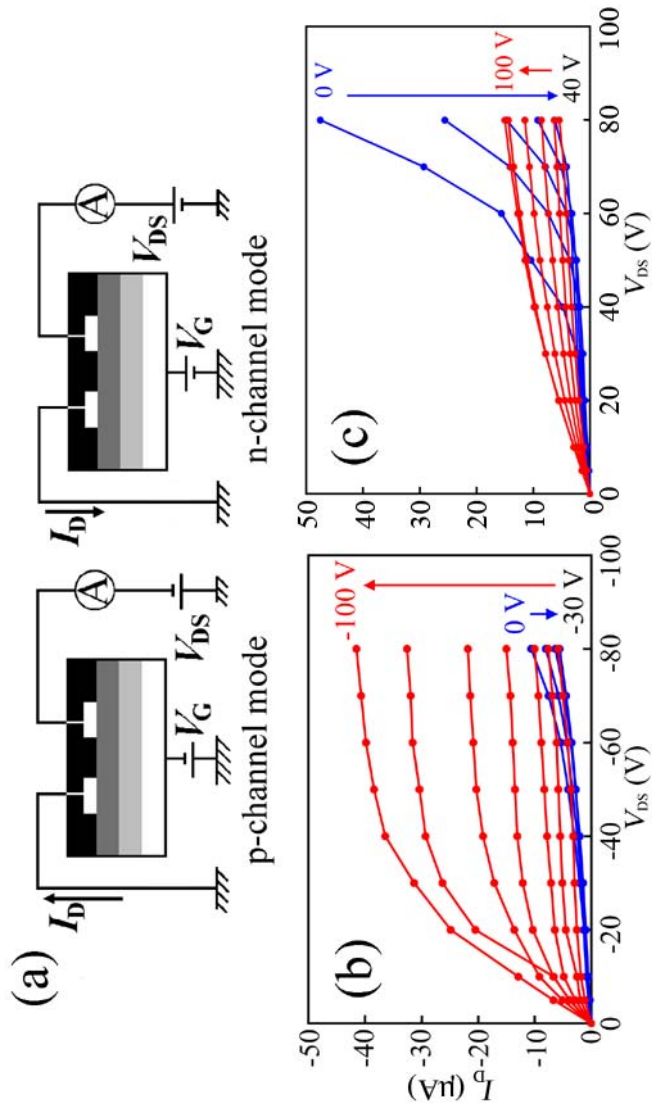


Fig. 2. E. Kuwahara et al.

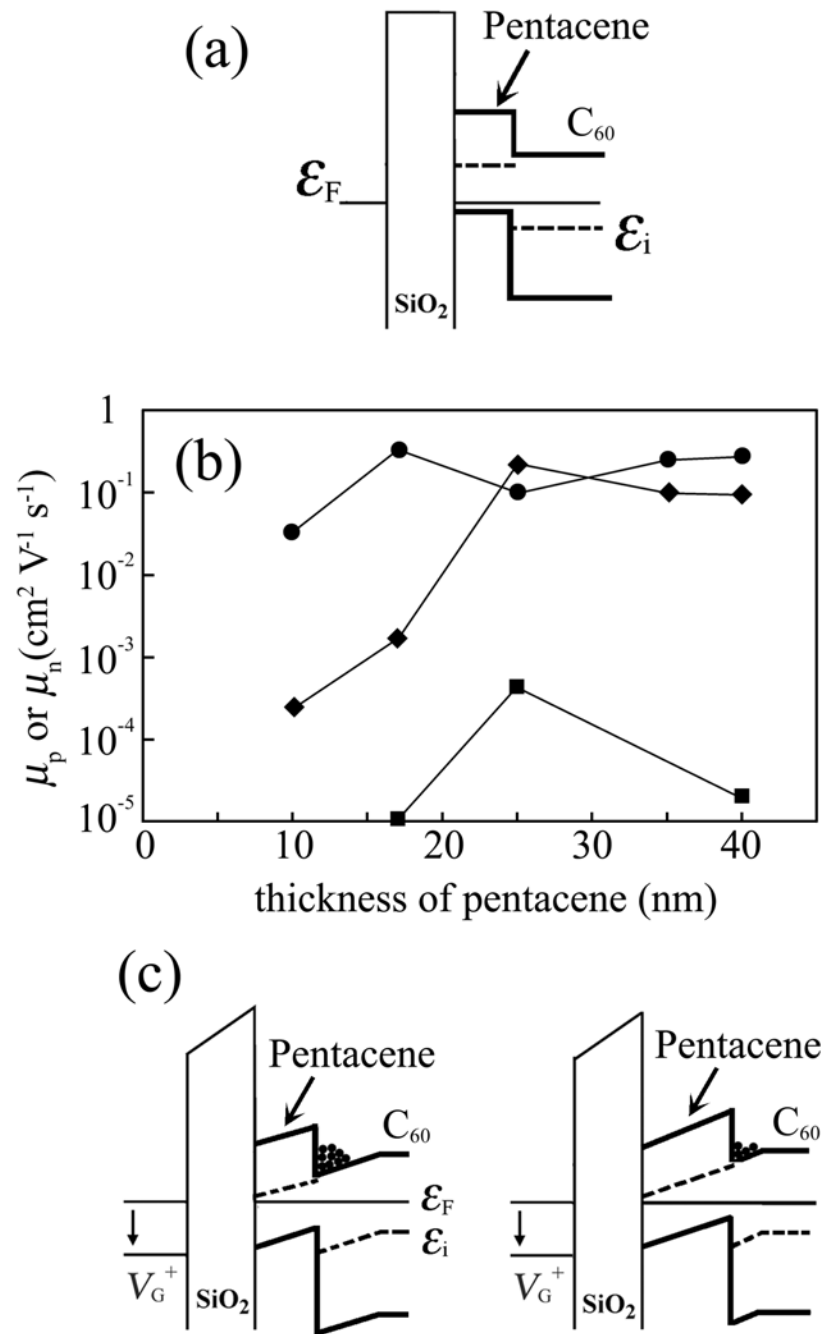


Fig. 3. E. Kuwahara et al.

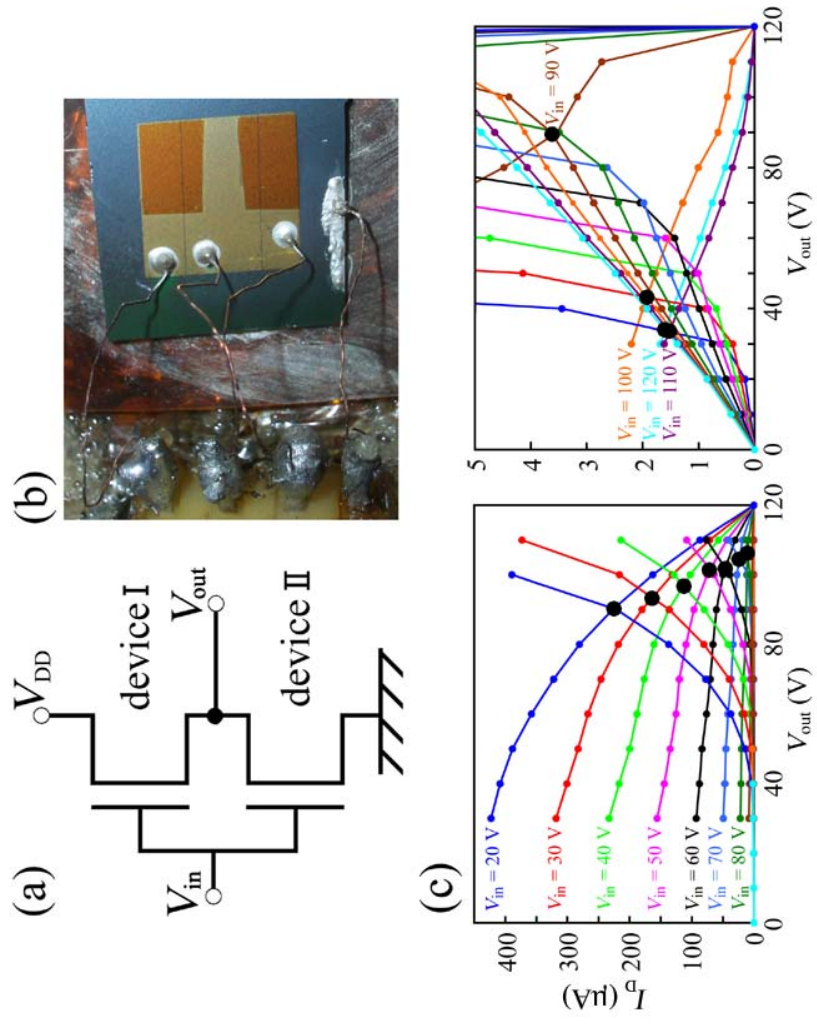


Fig. 4. E. Kuwahara et al.

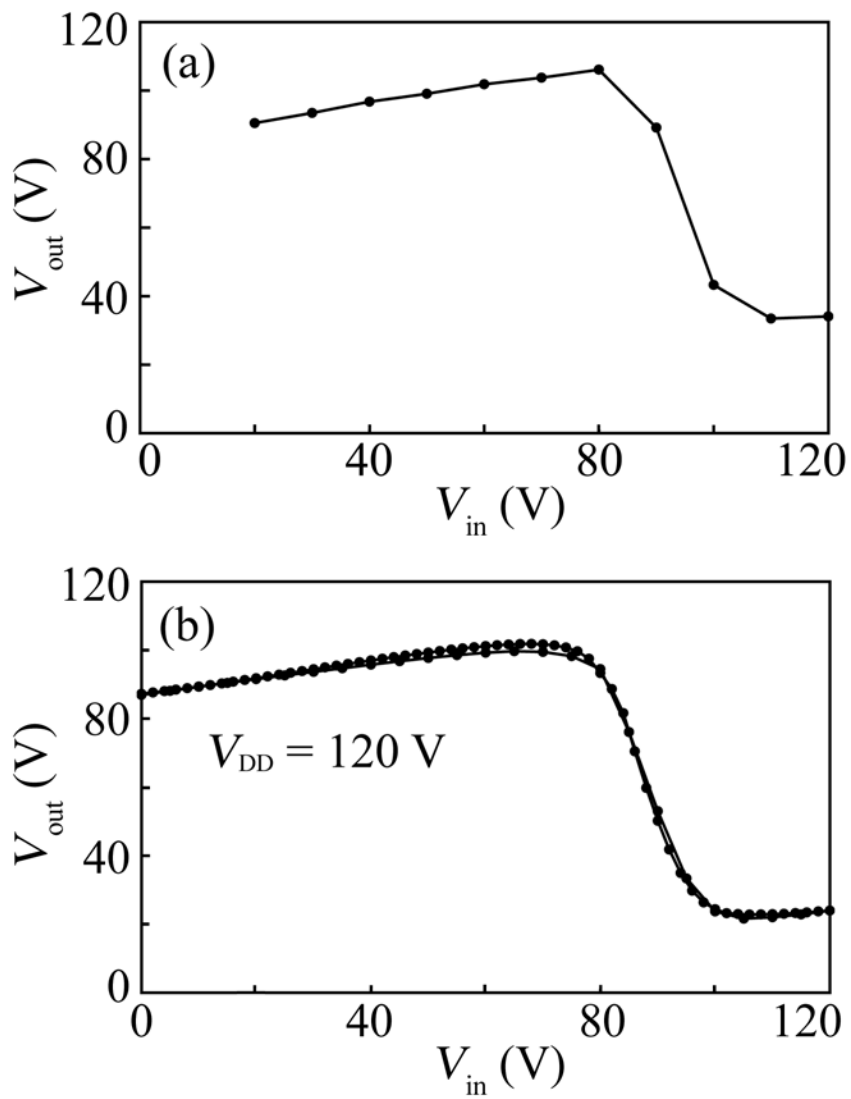


Fig. 5. E. Kuwahara et al.